A Systematically Generated, Pressure-Dependent Mechanism for High-Conversion Ethane Pyrolysis. 2. Radical Disproportionations, Missing Reaction Families, and the Consequences of Pressure Dependence

David M. Matheu*,† and Jeffrey M. Grenda‡

National Institute of Standards and Technology, Gaithersburg, Maryland 20899, and ExxonMobil Research and Engineering Company, Annandale, New Jersey 08801

Received: October 22, 2004; In Final Form: February 28, 2005

A previous, companion paper of this work (preceding paper in this issue) systematically developed a pressure-dependent reaction mechanism for the high-conversion pyrolysis of ethane,[1] as studied experimentally by Glasier and Pacey.[2] By combining conventional equilibrium, sensitivity, and reaction pathway analyses, that study identified a complex set of reaction pathways governing the formation and destruction of the important minor products acetylene, propylene, 1,3-butadiene, and benzene, which are pyrocarbon deposition precursors. To more confidently understand, and potentially manipulate, the complex chemistry governing deposition precursors, this work examines in more detail (1) the role of large sets of radical disproportionation reactions in forming the minor products, (2) the consequence of ignoring certain reactions during mechanism construction, (3) the appropriateness of the plug flow assumption used to model the reactor, and (4) the importance of reaction pressure dependence to the predictions of the minor product concentrations. We find that the predicted benzene concentration is sensitive to the presence of a specific, large collection of radical disproportionation reactions, typically neglected in most modeling efforts and of consequence only in the aggregate. Reaction families allowing Diels−Alder reaction, ene reaction, and triplet ethylene formation are safely ignored during model construction for the experimental conditions, but two specific reactions proposed in the literature, which rapidly convert fulvene to benzene, potentially explain the underprediction of benzene by the generated model. However, the rates proposed for these reactions are either unrealistically fast, or unconfirmed. We find the plug flow assumption reasonable in most respects, but its neglect of H-atom diffusion could explain the mechanism's systematic underprediction of hydrogen concentration at longer residence times. Finally, we demonstrate that accurate predictions of the minor product predictions appear to require the systematic treatment of pressure dependence employed by our mechanism generation algorithm. Changing the pressure in the experimental reactor alters the distribution of the minor products, or deposition precursors, through changes in the pressure-dependent reaction rates involved in their formation. We close with suggestions for the future development of automated mechanism generation tools, based on the current results.

1. Introduction

Part 1 of this work constructed the first systematically developed kinetic model for the high-conversion ethane pyrolysis system of Glasier and Pacey,[2] using the automated mechanism generation tool XMG-PDep.[1] Through combined equilibrium, sensitivity, and reaction pathway analyses, we identified sets of key pathways controlling the formation and destruction of the gas-phase minor products acetylene, propylene, 1,3-butadiene, and benzene, all of which are suspected pyrocarbon deposition precursors. While good agreement was achieved without numerical adjustment of parameters, the research raised many compelling questions.

First, in the original work, we noted the apparent importance of large collections of radical disproportionation reactions, especially for producing benzene from methylallyl radical (in our model, the methylallyl radical arises in quantity from the pressure-dependent addition of vinyl radical to ethylene). Here we focus on these reactions, examining in detail their effect on the predicted benzene concentration. We also study the general sensitivity of model predictions to the rate estimates used for the disproportionations of resonantly stabilized radicals, as these are among the most uncertain inputs to our automated kinetic model construction.

Second, our model construction effort in part 1 neglected a number of reaction families, or types, including Diels−Alder reactions, ene reactions, and triplet ethylene formation. We demonstrate here that neglect of these reaction types is generally justified for ethane pyrolysis conditions, as they have little effect on the model's structure or its predictions. Since the generated model underpredicts the observed benzene formation, we also study the ability of specific reactions—proposed in the literature but neglected by our generation algorithm—to bring the predicted benzene concentration closer to the experimental value.

Third, we probe the reasonableness and accuracy of the plug flow model used to represent the experimental reactor system in both works. Dimensionless parameter analyses and simplified 2-D reacting flow modeling show that the assumption of plug flow is generally reasonable, but that the neglect of axial H-atom diffusion may not be justified and could explain the

* To whom correspondence should be addressed. Present address: Cabot Corp., Billerica, MA 01821. E-mail: dmatheu@cabot-corp.com.
† National Institute of Standards and Technology.
‡ ExxonMobil Research and Engineering Co.

10.1021/jp0451647 CCC: $30.25
Published on Web 05/26/2005

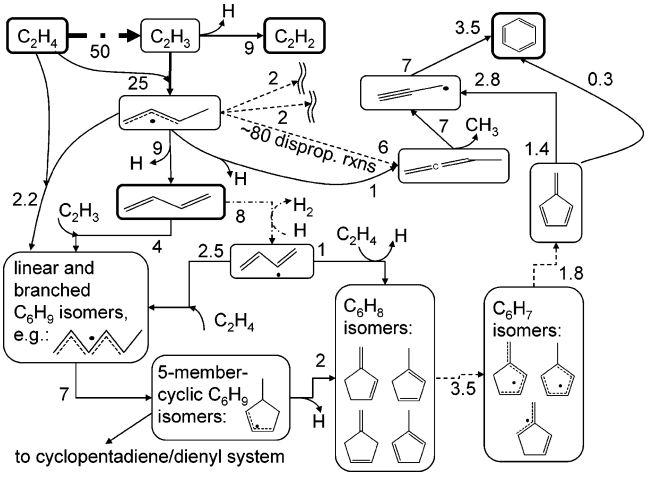

Figure 1. Partial pathway diagram for the production and consumption of minor products at the 5 s nominal residence time, same as Figure 12 in part 1.[1] Each arrow can represent a single pathway or a collection of parallel reaction pathways of the same general type. Solid lines are net pressure-dependent pathways. Dotted lines are radical disproportionation reactions or their reverse processes. Dashed−dotted lines are radical abstraction reactions. Numbers represent integrated, net molar flux from 7.5 to 30 cm, relative to C_2H_4 consumption (=100). Arrows with two sets of numbers reflect doubling due to stoichiometric coefficients, i.e., dissociation of fulvene to two propargyl radicals. Many pathways cannot be included in this diagram; Figure 13 of Part 1 shows some additional pathways.

underprediction of the hydrogen concentration in part 1 at slow flow rates.[1]

Finally, we demonstrate the specific importance of pressure dependence to the overall reaction mechanism by rebuilding the chemical kinetic model with the assumption that all pressure-dependent reactions proceed at the high-pressure limit. Furthermore, to show how pressure changes might be used to affect the minor product distribution, we model and predict the effect of a throttling valve placed midway through the high-conversion pyrolysis reactor. The results demonstrate how studies of intentional pyrocarbon deposition processes can benefit from explicit, systematically developed, pressure-dependent chemical kinetic models such as the one developed in this study and the companion work (preceding paper in this issue).

2. Sensitivity to Collections of Radical Disproportionation Reactions

2.1. Sensitivity to Rate Rules Used for Resonant-Radical Disproportionations. An important criticism of our companion paper (preceding paper in this issue) concerns the widespread presence of resonantly stabilized radical disproportionation reactions in the generated chemical kinetic model,[3], e.g.

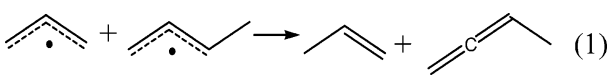

(1)

This subclass of radical disproportionation makes up a substantial fraction (about 1/2) of all the disproportionation reactions participating in Figure 1 (dotted-line pathways). XMG-PDep's rate rule for reactions of this subclass is the same as that used for all radical disproportionations:[4] a preexponential factor of 1.0×10^{12} cm^3/(mol s) per site, with the temperature exponential n and the reaction barrier E_a set to 0.

Some work suggests that disproportionations between resonantly stabilized radicals are far slower than this rate rule, if they occur at all.[5] That makes the rate constants used for resonantly stabilized radical disproportionations (and their reverse reactions) the most uncertain of all parameters in the work, with potential consequences for the predictions of the minor product concentrations.

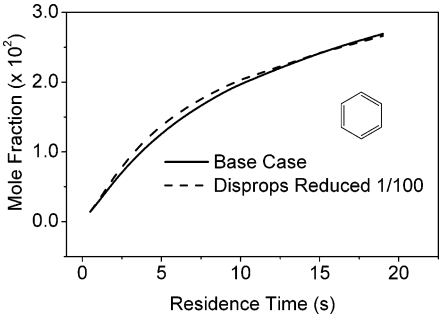

Figure 2. Predicted benzene concentration at the reactor outlet, for the original case (solid line) and with all disproportionation reaction rates between resonantly stabilized radicals reduced by a factor of 100 (dashed line). The predictions for both cases are similar, because with the resonant radical disproportionation pathways effectively removed, other pathways in the model emerge to maintain the same propargyl radical concentration, leading to nearly the same benzene concentration.

We developed a program to reduce *all* the resonantly stabilized disproportionation reaction rates in the mechanism (i.e., all analogues of eq 1) by a factor of 100, to test the predictions' sensitivity to these uncertain parameters. Rates for the corresponding reverse reactions were similarly reduced to maintain thermodynamic consistency. The result presented in Figure 2 for the benzene prediction is typical: for all the measured minor products except propylene, we find almost no difference between the original predictions and those with all resonant-radical disproportionations reduced by a factor of 100, despite the prevalence of this reaction type throughout the model.

In the case of benzene, three effects within the model combine to keep the predicted concentration the same despite the dramatic reduction of resonantly stabilized radical disproportionations. The primary route to benzene remains recombination of the propargyl radical, as shown in Figure 1, but the route from fulvene to propargyl becomes more important, and the route from 1,2-butadiene to propargyl becomes less significant. In addition, disproportionations of the methylallyl radical with more active radicals (e.g., H and CH_3) convert more methylallyl radical to 1,2-butadiene, which goes on to form propargyl; this helps maintain the pathway to propargyl radical discussed earlier.

Finally, the amount of propargyl radical consumed by disproportionation is drastically reduced; although not shown in Figure 1, propargyl radical in the original model participates in many resonantly stabilized radical disproportionations. Since both consumption and production fall with the effective removal of this reaction subclass, propargyl radical concentrations in the hot zone remain mostly unchanged. All these results suggest that the model predictions of the measured minor products are not very sensitive, as a whole, to the uncertainty of the global rate rule used for all resonantly stabilized radical disproportionations, even when it is changed by a significant factor.

2.2. Conversion of Methyallyl Radical to 1,2-Butadiene. Although, as demonstrated above, model predictions are largely insensitive to the *global* rate applied to resonantly stabilized radical disproportionations, certain predictions are still sensitive to the *presence* of *specific groups* of disproportionation steps, resonantly stabilized or not. To show this, we removed from the original model all disproportionations connecting methyallyl

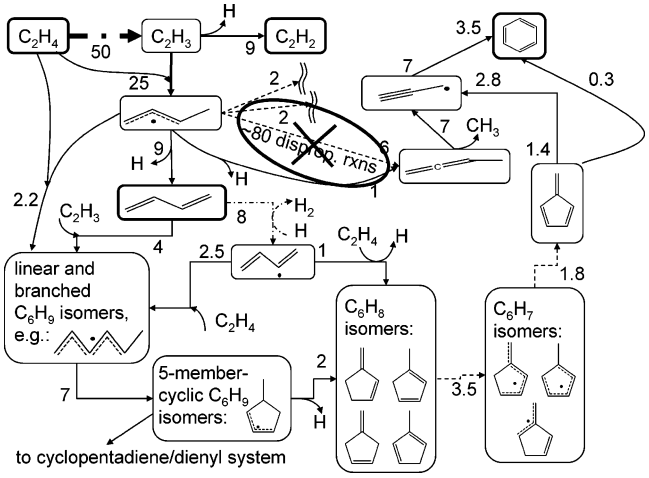

Figure 3. All the specific disproportionations and reverse disproportionations connecting methyallyl radical and 1,2-butadiene, removed to study the effects of these reactions on predicted benzene concentration.

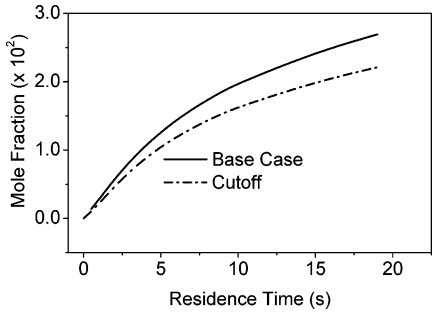

Figure 4. Predictions of benzene concentration from the original generated model (solid line) and with all disproportionation or reverse disproportionation reactions connecting methyallyl radical and 1,2-butadiene removed (dashed−dotted line). Removal of all 80 of these pathways causes a mild decrease in the predicted benzene concentration.

radical and 1,2-butadiene in Figure 1, as well as their reverse instances, as illustrated in Figure 3.

Removing this specific group of radical disproportionations lowers the predicted concentration of benzene by 25−30%, as shown in Figure 4. The altered prediction is farther from the experimental data than the original case, which was already an underprediction of benzene compared to the experimental value. We may conclude that, as a group, these disproportionations do matter to the model's prediction of benzene, though no individual reaction in the group exhibits strong sensitivity.

Although predicted benzene production is reduced, it is not eliminated; as expected, other pathways in the model partially compensate for the removal of the disproportionation set. The route through five-membered-ring cyclic species to fulvene, and then to propargyl radical, in Figure 1, becomes much more important, accounting for roughly 1/2 the propargyl radical formed. The 1,2-butadiene forms by a variety of other pathways, many of which were originally too slow to be displayed in Figure 1. In particular, the C_4H_5 radicals:

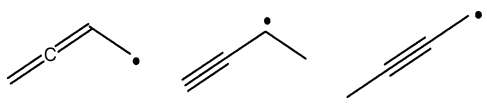

become sources for 1,2-butadiene by H-abstraction or disproportionation.

The mild sensitivity to the presence of disproportionations connecting methyallyl and 1,2-butadiene is a direct consequence of the many interconnected, parallel pathways to the various intermediates in the kinetic model. Artificially reducing one set of pathways will sometimes allow other pathways to emerge in importance. This strong interconnectedness of reaction pathways suggests that many of the intermediates in Figures 12 and 13 of part 1 may be governed by rate-constrained chemical equilibrium.[6−8] Some sets of intermediates are connected by so many reaction pathways that they equilibrate with each other, though their ultimate formation and consumption are kinetically limited (this situation occurs very frequently with large kinetic models).

3. Missing Reaction Families and Pathways

As noted earlier, XMG-PDep cannot, on its own, discover or consider concerted processes, diradical formation and consumption, or reactions involving electronically excited states.[9] While no generation tool could include all possible reaction families, the fact that certain families are missing from XMG-PDep could mean our generated model lacks important species and reactions. Below we estimate the consequences of neglecting three broad reaction families on the predicted concentrations of the observed minor products. We also study the effect of including a few, specific reactions from the literature that have been considered as important routes to benzene or other aromatics in combustion and pyrolysis systems.

3.1. Potential Effects of Neglected Reaction Families. *3.1.1. Triplet Ethylene Formation.* It has been suggested[10] that the lowest lying electronically excited triplet state of ethylene might be important under the Glasier and Pacey conditions, since it is only about 250 kJ/mol above the ground state. Furthermore, Gemein and Peyerimhoff's theoretical work suggests radiationless transitions between the excited and ground states are possible through a coupling with the vibrational modes.[11] Ethylene is a dominant species in the experiments, and formation of even a small amount of triplet ethylene could be important; this step would be chain-branching if triplet ethylene functioned as a diradical.

To understand whether, given a reaction family to represent the process, XMG-PDep would have identified triplet ethylene as kinetically significant, we compared the maximum possible production flux for triplet ethylene with the lowest values of the cutoff flux R_{min} (see ref 1). To estimate the needed rate constant for triplet ethylene formation, we started with Gemein and Peyerimhoff's suggestion that the rate constant for the reverse process—radiationless decay of the excited state to the ground state—would be approximately 10^6 to 10^8 s^{-1}. Using standard statistical thermodynamic relations and the results of our own B3LYP/6-31G* ab initio calculations, we estimated an upper bound for the rate constant of thermal formation of triplet ethylene from ground-state ethylene, at the reactor hot zone conditions, and used this value to estimate the maximum possible triplet ethylene production rate.

The results are presented in Table 1. Surprisingly, the production flux for triplet ethylene production exceeds the lowest value for the cutoff flux, which implies that the mechanism generation algorithm might have included triplet ethylene in the generated model (we have ignored any pressure dependence of the thermal process). But Table 1 also reflects the likely possibility that nearly all the triplet ethylene formed in this way would rapidly decay back to the ground state.

Furthermore, its equilibrium concentration would be so small that it could not perturb any of the predictions of the observed minor products, at least by the expected routes of radical abstraction or addition. To estimate this, we assumed triplet ethylene would function as a diradical, and could attack the

TABLE 1: Estimates of the Formation and Destruction Fluxes for Triplet Ethylene, and the Potential Effects on the Predictions of Some Minor Products, at 1200 K[a]

R_{min} (lower bound)	5.0E−09
triplet ethylene formation flux (upper bound)	4.3E−08
triplet ethylene equilibrium concn (mol/cm^3)	4.3E−16
consumption fluxes	
decay to ground state	4.3E−08
maximum loss by abstraction reactions	∼4.0E−11
maximum loss by addition reactions	∼4.0E−11
effects on minor products	
percent of net propylene production	0.02
percent of net 1,3-butadiene production	0.01
percent of net benzene production	0.05
percent of net acetylene production	0.03
effect on radical production	
percent of hot zone radical production	∼0.004

[a] Fluxes are in units of mol/(cm^3 s). The formation flux upper bound is greater than the lower bound of the R_{min} flux, so XMG-PDep would have "picked up" triplet ethylene. But further analysis suggests nearly all of the triplet ethylene would simply decay back to the ground state (consumption rates), and the low concentration of this species would prevent it from consuming a significant amount of the minor products discussed earlier. Finally, triplet ethylene formation would not be significant as a chain-branching step.

TABLE 2: Maximum Effect of Including Ene Reaction Families on the Fluxes of the Minor Products in the Reactor Hot Zone[a]

percent of net propylene production	3.3
percent of net 1,3-butadiene production	2.1
percent of net benzene production	1.9
percent of net acetylene production	1.7

[a] These values assume each double or triple bond in the minor product can react by ene reaction with all other unsaturated bonds in the model, at a rate equal to that for propylene + propylene. Even with this conservative estimate, ene reactions cannot provide an important consumption pathway for any of the minor products.

minor products by radical addition and H-abstraction, at rates equal to our rate rules for vinyl radical abstraction and addition.

Radical production rates, or chain-branching effects, of the single reaction of ground-state ethylene forming triplet ethylene, are also small compared to the overall system's rate of radical production. All of this implies that although the XMG-PDep algorithm would discover triplet ethylene, the triplet ethylene concentration (even at equilibrium with ethylene) would be too small to be important to the system.

3.1.2. Ene and Retro-Ene Reactions. Ene reactions and their reverse processes, retro-ene reactions, are well-known concerted pathways available to hydrocarbon molecules, for example

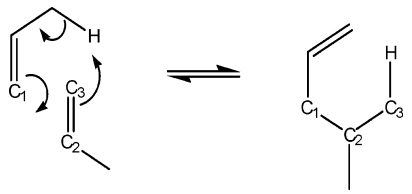

While it is impossible to fully judge the impact of including ene and retro-ene reaction families in the algorithm without actually building the family into the mechanism generation algorithm, we can show that such reaction pathways cannot, directly, affect the concentrations of the minor products. If ene reactions proceed with a rate constant similar to that for propylene + propylene,[12] then the total direct effect on the principle minor products would be as shown in Table 2. Even with the generous assumption that all unsaturated bonds were available to react with the minor product, as ene or enophile, none of these fluxes would strongly affect the net production rate of the minor products. Additionally, no ene reaction product would have a flux larger than the lower bound cutoff flux R_{min}, so the mechanism generation algorithm would not discover additional species this way.

Retro-ene reactions *would* strongly affect the concentration of any linear C_6H_{12} or C_5H_{10} olefin in the model, and would be the dominant consumption pathway for these species. Fortunately, none of these species are important minor products or intermediates, and none of them appear in any of the earlier reaction-pathway or sensitivity analyses.[1] There is a possibility, however, that important species in Figure 1, such as the five-membered-ring C_6H_8 isomers, could undergo inter- or intramolecular retro-ene reactions. Although these processes would appear to involve strained transition states (and therefore be too slow to be important), we cannot eliminate the possibility of important retro-ene decompositions or isomerizations of these intermediates. Similarly, their ene reaction counterparts could form the important C_6H_8 intermediates from smaller species present in the model.

3.1.3. Diels−Alder and Retro-Diels−Alder Reactions. Diels−Alder reactions have been proposed in the past as alternative pathways to cyclic species (see, e.g., ref 13). Under our conditions, the most important Diels−Alder formation pathway would probably be the reaction of ethylene with 1,3-butadiene:

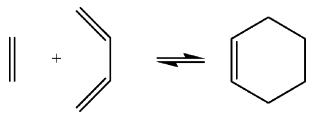

Skinner and co-workers[14] measured the gas-phase rate constant for the reverse of this reaction (cyclohexene decomposition to ethylene and 1,3-butadiene) at high pressure and temperatures from 1000 to 1340 K. Using these data, a calculation of the equilibrium constant, and calculation of the pressure-dependent rate constants at the experimental conditions, we found that the flux of the Diels−Alder reaction of ethylene and 1,3-butadiene in the hot zone would be $\sim 4 \times 10^{-9}$ mol/(cm^3 s). This value is almost equal to the lowest value of R_{min} discussed earlier. Therefore, XMG-PDep might have included cyclohexene in the generated model, formed by this pathway, if Diels−Alder reaction families had been part of the algorithm. However, as is the case for triplet ethylene, cyclohexene decay would be dominated by the reverse process, retro-Diels−Alder reaction. This process is 3 orders of magnitude faster than the fastest conceivable rates of small radical attack (via addition or abstraction) on cyclohexene.

Because cyclohexene would rapidly re-form ethylene and 1,3-butadiene at the experimental conditions, the Diels−Alder reaction family would not perturb the 1,3-butadiene concentration. Analogous consumption of propylene, acetylene, or benzene by such reactions would have even less impact on the concentrations of these minor products. The possibility remains that some cyclohexene would undergo radical attack to initiate another pathway to aromatic species in the model, but this pathway would probably be of minor importance.

3.2. Missing Reactions Forming Benzene and Other Aromatics. There are many individual reactions which have been suggested over the years as possible routes to benzene or other aromatics under conditions similar to those of Glasier and Pacey. Some of these additional reactions pass through unknown transition states, so XMG-PDep could not discover these. Others involve complex diradical intermediates or concerted steps, which are inaccessible for XMG-PDep's algorithm. A few

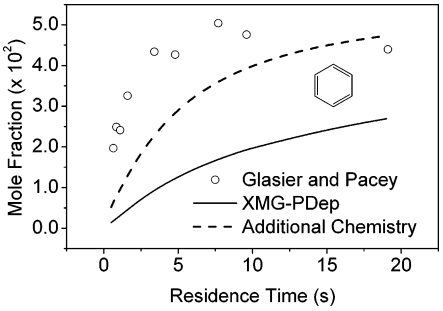

Figure 5. Predicted benzene concentration from the original generated model (solid line) and with additional reactions from various literature sources added by hand (dotted line). The additional chemistry, which could not be explored by XMG-PDep, is a possible explanation for the benzene discrepancy, but the literature rates for the key additional reactions are questionably fast.

reactions are based only on the empirical evidence that some series of intermediates may connect the reactants and products.

Since XMG-PDep was unable to discover any of these reactions, we examined the effects of adding a selection of them to the generated model. The added reactions were drawn from various literature collections[15−17] and broadly include (1) cyclopentadienyl reactions with methyl, acetylene, or itself, to form phenyl radical, naphthyl radical, or naphthalene, (2) phenyl and benzyl radical formation and destruction reactions, including cyclohexadiene chemistry, (3) various concerted reactions not covered earlier, such as vinylacetylene addition to acetylene to form benzene, and (4) two "fast" reactions or pathways in the literature which are claimed to rapidly form benzene from fulvene[18,19] and which do not appear to be those given by Miller and Klippenstein.[20]

We caution that the pressure dependence of the rate constants for many of these added reactions is either entirely ignored or tuned to a specific pressure different from that of Glasier and Pacey. Figures 5 and 6 show the results of including these reactions in the generated model.

Figures 5 and 6 suggest that the underprediction of benzene and the incorrect trend in hydrogen concentration at longer residence times could be explained by additional chemistry which XMG-PDep has not explored. In fact, of all the added reactions, we find that only the two "fast fulvene" pathways

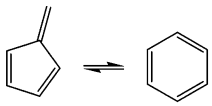

($A = 3\times10^{13}$ s^{-1}, $E_a = 278$ kJ/mol, ref.[19])

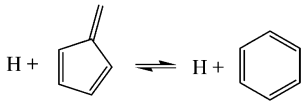

($A = 3\times10^{12}$ cm^3/mol-s-K^n, $n = 0.5$, $E_a = 8.4$ kJ/mol, ref.[18])

are the ones responsible for raising the predicted benzene concentration in Figure 6. If XMG-PDep had the appropriate reaction families, its discovery of these reactions would have provided another route to benzene.

We question the proposed rate constants for both of these reactions, however. The first, for direct fulvene−benzene isomerization, derives from a very low pressure pyrolysis (VLPP) experiment.[19] In the analysis to determine the rate constant, the reaction was assumed to pass through a hypothetical transition state which (to our knowledge) has never been identified by ab initio calculation; furthermore, the work

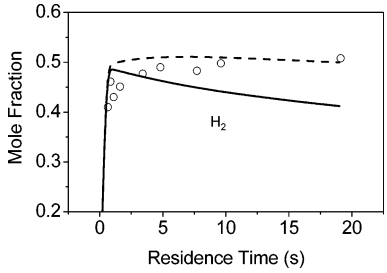

Figure 6. Hydrogen concentration prediction from the original generated model (solid line) and with additional reactions added (dotted line).

represents the only experimental study of a direct fulvene-to-benzene isomerization[20] and is unconfirmed by any other experimental studies.

The rate constant suggested by Marinov and co-workers for the second reaction,[18] a multistep isomerization resulting from the chemically activated addition of H-atom to a fulvene double bond, is based on an earlier ab initio (BAC-MP4) potential energy surface calculation.[21] But the derived rate is 2 times faster than the *high-pressure limit* for H-atom radical addition to ethylene at 1100 K,[22] and 4−10 times faster than the high-pressure-limit addition rates of H-atom to double bonds as reported in many other detailed studies, including H-atom addition to the benzene double bond.[12,23,24] A multistep, chemically activated isomerization *cannot* occur faster than the high-pressure limit of the first step.

Neither of these are reflections of the fulvene-to-benzene isomerization discussed in Miller and Klippenstein,[20] which we included in the original mechanism. Thus, while Figure 5 clearly shows that additional reactions *could* explain the benzene concentration underprediction, more research is required to confidently suggest the proposed additional reaction pathways above as good explanations.

The hydrogen concentration in Figure 6 reflects the increase in benzene formation, because the boost in benzene concentration allows more hydrogen to form. As discussed in the next section, however, H-atom diffusion may also explain the original model's discrepancy in the hydrogen concentration.

4. Plug Flow Model

Throughout our analyses we assume a plug flow model adequately describes the Glasier and Pacey experimental reactor, to make the modeling problem tractable. The plug flow model neglects the effects of axial conduction and diffusion, assumes that temperature, species concentrations, and flow velocities are all radially uniform, and ignores buoyancy-driven convection. This section tests these flow assumptions; details of the dimensionless parameter calculations may be found in the Supporting Information.

4.1. Axial Conduction and Diffusion. The neglect of species diffusion and heat conduction along the length of the reactor will have the strongest impact at the slowest experimental flow rates modeled. For axial heat conduction, we estimated a thermal Péclet number (*Pe*) of ∼0.8 at the slowest experimental flow rate (the Péclet number represents the ratio of axial heat convection, or bulk flow heat transport, to axial heat conduction). $(Pe)\lambda$, or the Péclet number multiplied by the ratio of reactor length to diameter, is then approximately 30. Axial conduction can usually be neglected when $(Pe)\lambda > 50$,[25] so the slowest flow rate is not quite fast enough to justify this assumption. However, at typical flow rates (e.g., the 5 s residence time), $(Pe)\lambda > 100$, so this aspect of the plug flow model is reasonable for most of the modeled range. We cite the good agreement of

C_2H_6, C_2H_4, and CH_4 concentration predictions with the experimental data, even at the slowest flow rate, as further justification that the consequences of ignoring axial conduction are not serious.

Péclet numbers for axial species diffusion are similar, with a value for a typical small species (C_2H_4) of about 0.7, at the slowest flow rate. This gives $(Pe_{C_2H_4})\lambda \approx 27$. The low value implies that, at slow flow rates, axial diffusion becomes competitive with bulk convection in the experimental reactor. However, as for axial heat conduction, at more typical experimental flow rates, we find $(Pe_{C_2H_4})\lambda \approx 100$ or greater. Once again, the good, unadjusted agreement found in our earlier work for C_2H_6, C_2H_4, and CH_4 concentrations[1] implies that, even at slow flow rates, the neglect of axial species diffusion in the reactor model does not impair overall accuracy.

The diffusion coefficient of the hydrogen atom, however, is greater than that for most small species by at least an order of magnitude. Using the Wang and Law estimate for the H-atom diffusion coefficient,[26] we found $(Pe_{H-atom})\lambda \approx 4$ at the slowest experimental flow rate, and only 35 at the fastest. Neglect of H-atom diffusion, though necessary to make the modeling problem tractable, may explain the underprediction of H_2 in Figure 4 of our companion paper (preceding paper in this issue),[1] as H-atoms at high concentration in the center of the reactor could be diffusing toward the lower concentrations in the reactor exit. This would generate more H_2 as the H-atoms abstracted available hydrogens from the other major products.

4.2. Radial Uniformity of Temperature, Species Concentrations, and Velocities. In the Pacey and Glasier experiments, cold fluid is fed into a reactor with hot walls, so that fluid near the wall is heated first. But the narrow tube diameter ensures that temperatures rapidly become radially uniform, even at the fastest experimental flow rates. We estimated a thermal entrance length of ~0.3 cm,[25,27] which implies that the fluid flowing near the reactor centerline experiences an increase in temperature within a centimeter of the reactor entrance. We tested this assumption using a 2-D flow simulation tool,[28,29] which, although it ignores axial diffusion and conduction, rigorously treats radial heat and mass transfer. The 2-D flow modeling results confirmed the entrance length calculation, and demonstrated that, even at the fastest experimental flow rate, the fluid temperature is radially uniform (within 5%) after 1.5 cm of the entrance, or less than 1/20 of the full reactor length.

The overall reaction in the experiments

$$C_2H_6 \rightarrow C_2H_4 + H_2$$

is endothermic, and by absorbing energy could extend the thermal entrance length and promote formation of a thermal boundary layer. To test whether reaction endothermicity could strongly affect temperature uniformity, we constructed a simplified chemical kinetic model, based on the full generated model, with 9 species and 13 reactions. We used this mechanism with the 2-D flow model and examined the temperature profiles. Results suggested that, even with the overall endothermic reaction, the system achieves radial temperature uniformity (within 5%) beyond 2.5 cm, slightly longer than our earlier calculation, but still short compared to the reactor length of 40 cm.

In contrast to the analysis of temperature uniformity, the 2-D flow model shows that, at the fastest flow rate, some species concentration profiles are not radially uniform until the middle of the reactor hot zone (about 20 cm). But comparison of the 2-D model with a plug flow model using the same simplified chemical mechanism showed differences of less than 5% for species concentration predictions at the reactor exit, implying that small-scale species nonuniformity did not affect the model predictions.

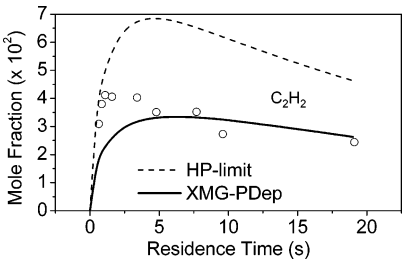

Figure 7. Predicted acetyelene concentration from the XMG-PDep-generated model in the original case (solid line) and with pressure-dependent reactions forced to behave as if they were in the high-pressure limit (dashed line). The falloff for small-molecule reaction rate constants (such as vinyl decomposition to acetylene + H-atom) was preserved.

Finally, the Reynolds number (*Re*) for all flow rates modeled in this work is about 10 or less, indicating parabolic, and not flat, velocity profiles. The 2-D reacting flow model incorporates momentum transfer and employs a true parabolic velocity profile, instead of the flat profile assumed by the plug flow model. We cite the above agreement between the 2-D reacting flow model and the plug flow model to suggest that our assumption of a flat profile was reasonable at all experimental flow rates.

4.3. Natural Convection. Natural, or buoyancy-driven, convection is a potential concern at the slower flow rates, especially given the vertical orientation of the reactor. Our estimation of the Grashof number (*Gr*), combined with the flow-regime charts of ref 27, suggests that, at most experimental conditions, the real flow is mixed between forced laminar and natural convection. The consequences of omitting natural convection effects in our reactor model are not clear. As justification for ignoring natural convection, however, we point to visual, experimental evidence in later work by Glasier and Pacey,[30] which suggested that, even at the lowest flow rates, natural convection was not significant.

5. Importance of Pressure Dependence

5.1. Pressure-Dependent Pathways to the Minor Products. Despite the interconnectedness of reaction pathways and the availability of alternate routes to nearly all the minor products, the treatment of reaction pressure dependence strongly affects the model predictions. To show this, we regenerated the chemical kinetic model, forcing nearly all automatically discovered pressure-dependent reactions to be in their high-pressure limit. We did preserve the pressure dependence of small-molecule pathways, e.g.

$$C_2H_5 \rightleftharpoons C_2H_4 + H$$

since no sincere modeling effort would be able to ignore the falloff in such reactions at the Glasier and Pacey conditions. The pressure-dependent rate constants for the propargyl + propargyl system, taken directly from Miller and Klippenstein,[20] were also preserved.

Figures 7−11 suggest that proper treatment of the pressure dependence is, in fact, crucial to the prediction of the minor species concentrations at the Glasier and Pacey conditions. Predictions without systematic pressure dependence differ from those of the original case by factors of 2 or 3, almost always farther from the experimental data. In some instances, the overall shape is also incorrect (e.g., ethane, propylene, and benzene).

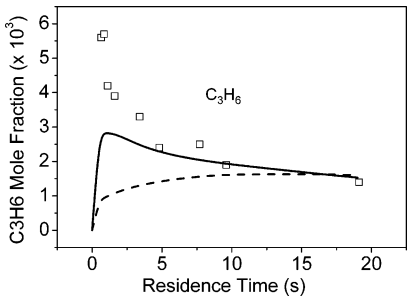

Figure 8. Predicted propylene concentration from the XMG-PDep-generated model in the original case (solid line) and with pressure-dependent reactions forced to behave as if they were in the high-pressure limit (dashed line).

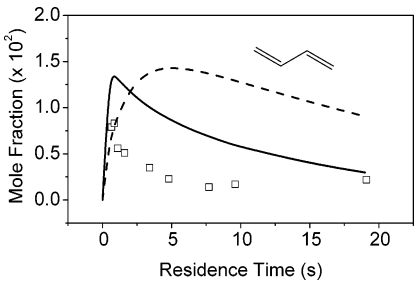

Figure 9. Predicted 1,3-butadiene concentration from the XMG-PDep-generated model in the original case (solid line) and with pressure-dependent reactions forced to behave as if they were in the high-pressure limit (dashed line).

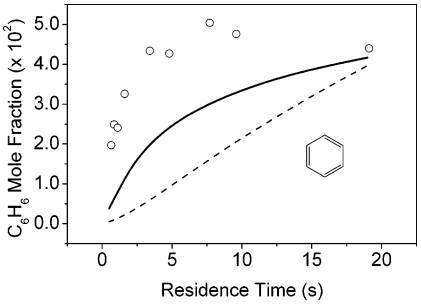

Figure 10. Predicted benzene concentration from the XMG-PDep-generated model in the original case (solid line) and with pressure-dependent reactions forced to behave as if they were in the high-pressure limit (dashed line).

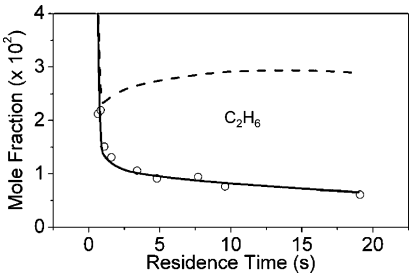

Figure 11. Predicted ethane concentration from the XMG-PDep-generated model in the original case (solid line) and with pressure-dependent reactions forced to behave as if they were in the high-pressure limit (dashed line).

This result fits well with the presence of many pressure-dependent pathways in Figure 1, and with the earlier results of Wong that large-molecule reacting systems still exhibit strong pressure dependence.[31] The major product concentrations (methane, hydrogen, ethylene) were not strongly affected by forcing pressure-dependent reaction rate constants to the high-pressure limit.

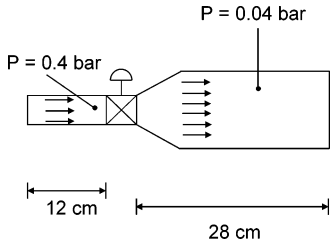

Figure 12. Theoretical redesign of the Glasier and Pacey experimental reactor which lowers pressure to 1/10 the original experimental pressure, beyond 1/3 of the reactor length (12 cm). In this design the throttling is isenthalpic, such that the temperature is unperturbed, assuming the gas is ideal. The reactor diameter in the first section is 1.0 cm; beyond the throttling valve, it must be 3.2 cm (or $\sqrt{10} \times 1$ cm) for the gas speeds in both sections to match. This is a condition of isenthalpic throttling.

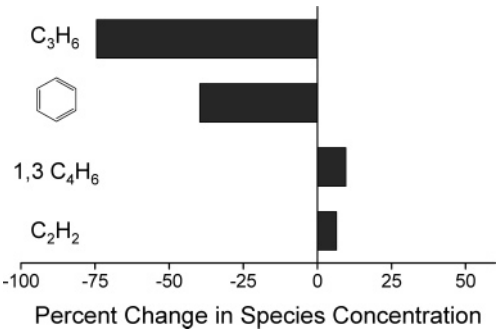

Figure 13. Changes in the reactor exit product distribution of the throttled reactor compared to the original case. The throttling process boosts selectivity to ethylene, while lowering selectivity for benzene and propylene, and leaving acetylene and 1,3-butadiene mostly untouched; in other words, throttling is able to effectively change the mix of minor products in the gas phase.

5.2. Changing the Minor Product Distribution by Changing Pressures. If the generated model predictions are truly sensitive to pressure, then changing the experimental reactor design to allow a pressure drop should produce significant changes in the gas-phase product concentrations. These changes could, in turn, alter the type of pyrocarbon deposited, and the rate of deposition. However, it is difficult to predict the change in gas-phase concentrations for a new geometry and pressure profile, without a kinetic model appropriate to the conditions. To demonstrate the potential power of our tool to explore reactor design changes, and to learn whether a particular design change could really affect the product yields, we imagined a redesign of the Glasier and Pacey reactor which includes a constant-temperature throttling to 1/10 the original pressure, as shown in Figure 12 (constant-temperature, or isenthalpic, throttling is described in many thermodynamics textbooks; see, e.g., ref 32).

We simulated the reactor in Figure 12 at a flow rate of 484 μg/s, by using two separate kinetic models. The original generated kinetic model (for 0.4 bar and 900−1200 K) was used for the first 12 cm, or the first third of the reactor length. XMG-PDep constructed an appropriate new model, at 1/10 this pressure (0.04 bar), for the section of the reactor beyond the throttle. We simulated both sections separately, with the predicted concentrations at the end of the first section taken as inlet concentrations for the second section. The temperature profile was identical to that used in the original case.

Figure 13 compares the predicted exit concentrations of the modified reactor with those of the original reactor at the same mass flow rate. The change in pressure has caused substantial changes in the relative yields of the minor products and especially of benzene and propylene. The new design has

reduced the yield of benzene and propylene, leaving 1,3-butadiene and acetylene relatively unchanged.

While a thorough analysis of the lower pressure model is beyond the scope of this work, we note that three major effects combine to produce the changes in product concentration predictions. First, new reaction pathways, different from those found previously, become important for the low-pressure section. Second, all pressure-dependent rate constants $k(T,P)$ are different at the lower pressure, sometimes substantially. Third, the throttling to lower pressure causes a dilution of all species concentrations, and this affects the fluxes of bimolecular and unimolecular reactions differently. The result of all these changes is extremely difficult to predict, without the benefit of a systematically developed model suited to the changed conditions.

Experimental results would of course be required to confirm the predictions of this section. But our results here suggest that, first, reactor design changes could change minor product concentrations in this system and, second, prediction of those changes requires an appropriate pressure-dependent kinetic model. Changing the precursor distribution could in turn alter the nature of the deposited pyrocarbon, and its rate of deposition.[33]

6. Conclusions

Disproportionation reactions between resonantly stabilized radicals appear to play an important role throughout the high-conversion pyrolysis reactions considered in the current work, yet their rate constants are the most uncertain of all parameters used by this study. Predicted species concentrations showed little sensitivity to the global rate rules used for all resonantly stabilized disproportionation reactions. In contrast, the benzene concentration *is* sensitive to the presence of a specific set of approximately 80 disproportionation reactions which convert methyallyl radical into 1,2-butadiene in Figure 1. In both cases, the complex nature of interconnected and parallel reaction pathways suggests that only experiments which specifically target disproportionations or their reverse reactions can help resolve the question of the true importance of such reactions to benzene or other minor products.

Triplet ethylene formation, Diels−Alder reactions, and ene reactions are not likely to play an important role at the conditions of the Glasier and Pacey experiments, so they are safely neglected in all parts of this work. The absence of two specific reactions reported in the literature, both of which rapidly convert fulvene directly to benzene,[18,19] could explain the generated model's underprediction of benzene and hydrogen concentrations at longer residence times. But the proposed rate constant for one of these reactions is so fast as to appear inconsistent with much other rate data on H-atom addition to double bonds. The other rate constant is the isolated result of a single, VLPP experiment and awaits confirmation by further experiment and ab initio modeling. Thus, it remains unclear whether either of these reactions can legitimately explain that portion of benzene production not included by the generated model.

This work assumed the Glasier and Pacey reactor operated as a plug flow system, with radial uniformity in temperature and species concentration, no natural convective flow, and no axial diffusion. Modeling of a trial system using a simplified reactive flow simulation package supports the assumptions of the plug flow model, and specific observations imply natural convection was not significant in this system. But dimensionless parameter analysis suggests that, at the lower flow rates, axial diffusion of the H-atom was competitive with the convective flow. Neglect of this phenomenon could explain the systematic underprediction of hydrogen in the generated model.

The mechanism generation algorithm's systematic and general treatment of pressure dependence proved critical to the prediction of the minor product, or deposition precursor, concentrations. Our modeling results suggest that a deliberate pressure change, such as the use of a throttling valve, could alter the deposition precursor distribution. If, as claimed previously, the nature of the deposited pyrocarbons depends in part on this distribution,[33] then such changes could be used to manipulate the deposited material quality.

The combined papers in this work reveal a highly complex gas-phase reaction network for high-conversion pyrolysis, one which is far from equilibrium, although some intermediates are in partial equilibrium with each other. The systematic quality of the mechanism construction algorithm suggests that this complexity reflects that of the real, natural system, and is what chemists should expect given our knowledge of the reactions of hydrocarbons. The effects of pressure, and pressure changes, in this complex system would be almost impossible to predict manually; our tool is the first, and currently the only, mechanism generation algorithm which can systematically investigate pressure changes in complex gas-phase reacting systems.

7. Future Directions

The above results suggest that radical disproportionation reactions, pathways to benzene in high-conversion pyrolysis, and the use of pressure to change the minor product distribution remain interesting questions for research. In addition to these directions, we suggest two helpful future developments for the large-scale kinetic modeling of complex systems. First, even with the flux termination criteria, the XMG-PDep algorithm and related tools generate a very large number of species and reactions. The conventional techniques we used to analyze the model are critical, but are also cumbersome, and their results must be combined to provide a coherent picture of the system. A systematic, or algorithmic, way of implementing rate-controlled chemical equilibrium techniques,[6,7] or other analysis strategies, online during mechanism generation, would be useful. Strictly mathematical reduction of the number of required computational cycles to solve the model is not sufficient for this purpose; there is a need for a tool that delivers a conceptual, chemical understanding as the complex generated model unfolds, because it is typically this understanding which guides process design.

The issue of uncertainties in the rate constants and thermochemical parameters—whether from the literature or from rate rules and estimation methods—has not been systematically addressed in this study. Advanced uncertainty propagation techniques, such as those of Tatang,[34,35] or other stochastic response surface methods, would be extremely helpful in understanding the generated model's predictions. In our simulation of an imagined reactor redesign, for example, a serious question is how certain we are that the minor product concentrations would actually change in the predicted directions, given the uncertainties in all the estimated parameters. The integration of advanced uncertainty analysis and large-scale kinetic model development remains key for the advancement of gas-phase kinetic models and their associated tools, such as XMG-PDep.

Acknowledgment. We thank Prof. William H. Green, Jr. of the Massachusetts Institute of Technology for the use of computing facilities, as well as providing thoughtful discussion and advice. Prof. Philip D. Pacey of Dalhousie University and

Dr. Greg Glasier of Wyeth Research supplied technical commentary and detailed information on their experiments. The advice and recommendations of Prof. Anthony M. Dean (Colorado School of Mines) and Dr. Wing Tsang (National Institute of Standards and Technology) are gratefully acknowledged. D.M.M. expresses gratitude to the National Research Council for funding.

Supporting Information Available: Details of the dimensionless parameter calculations. This material is available free of charge via the Internet at http://pubs.acs.org.

References and Notes

(1) Matheu, D. M.; Grenda, J. M. *J. Phys. Chem. A* **2005**, *109*, 5332−5342.

(2) Glasier, G. F.; Pacey, P. D. *Carbon* **2001**, *39*, 15−23.

(3) Tsang, W. (National Institute of Standards and Technology). Personal communication, 2004.

(4) Dahm, K. Hydrocarbon Pyrolysis: Experiments and Graph Theory Modeling. Ph.D. Thesis, Massachusetts Institute of Technology, Cambridge, MA, 1998.

(5) Tsang, W.; Walker, J. A. *J. Phys. Chem.* **1992**, *96*, 8378−8384.

(6) Keck, J. C.; Gillespie, D. *Combust. Flame* **1971**, *17*, 237−241.

(7) Keck, J. C. *Prog. Energy Combust. Sci.* **1990**, *16*, 125−154.

(8) Tang, Q.; Pope, S. B. *Proc. Combust. Inst.* **2003**, *29*, 1411−1417.

(9) Matheu, D. M.; Dean, A. M.; Grenda, J. M.; Green, W. H., Jr. *J. Phys. Chem. A* **2003**, *107*, 8552−8565.

(10) Irikura, K. K. (National Institute of Standards and Technology). Personal communication, 2004.

(11) Gemein, B.; Peyerimhoff, S. D. *J. Phys. Chem.* **1996**, *100*, 19257−19267.

(12) Tsang, W. *J. Phys. Chem. Ref. Data* **1991**, *20*, 221−273.

(13) Sakai T. In *Pyrolysis: Theory and Industrial Practice*; Albright, L. F., Crynes, W. L., Corcoran, W. H., Eds.; Academic Press: New York, 1983; pp 89−116.

(14) Skinner, G. B.; Rogers, D.; Patel, K. B. *Int. J. Chem. Kinet.* **1981**, *13*, 481−495.

(15) Skjoth-Rasmussen, M. S.; Glarborg, P.; Ostberg, M.; Johannessen, J. T.; Livbjerg, H.; Jensen, A. D.; Christensen, T. S. *Combust. Flame* **2004**, *136*, 91−128.

(16) Appel, J.; Bockhorn, H.; Frenklach, M. *Combust. Flame* **2000**, *121*, 122−136.

(17) Richter, H.; Howard, J. B. *Phys. Chem. Chem. Phys.* **2002**, *4*, 2038−2055.

(18) Marinov, N. M.; Pitz, W. J.; Westbrook, C. K.; Vincitore, A. M.; Castaldi, M. J.; Senkan, S. M.; Melius, C. F. *Combust. Flame* **1998**, *114*, 192−213.

(19) Gaynor, B. J.; Gilbert, R. G.; King, K. D.; Harman, P. J. *Aust. J. Chem.* **1981**, *34*, 449−452.

(20) Miller, J. A.; Klippenstein, S. J. *J. Phys. Chem. A* **2003**, *107*, 7783−7799.

(21) Melius, C. F.; Colvin, M. E.; Marinov, N. M.; Pitz, W. J.; Senkan, S. M. *26th Symp. (Int.) Combust.* **1996**, *26*, 685−692.

(22) Baulch, D. L.; Cobos, C. J.; Cox, R. A.; Frank, P.; Hayman, G.; Just, T.; Kerr, J. A.; Murrells, T.; Pilling, M. J.; Troe, J.; Walker, R. W.; Warnatz, J. *J. Phys. Chem. Ref. Data* **1994**, *23*, 847−1033.

(23) Davis, S. G.; Law, C. K.; Wang, H. *J. Phys. Chem. A* **1999**, *103*, 5889−5899.

(24) Baulch, D. L.; Cobos, C. J.; Cox, R. A.; Esser, C.; Frank, P.; Just, Th.; Kerr, J. A.; Pilling, M. J.; Troe, J.; Walker, R. W.; Warnatz, J. *J. Phys. Chem. Ref. Data* **1992**, *21*, 411−734.

(25) Deen, W. M. *Analysis of Transport Phenomena*; Oxford University Press: New York, 1998.

(26) Wang, H.; Law, C. K. Diffusion Coefficient of Hydrogen Atom for Combustion Modeling. *1996 Technical Meeting of the Eastern States Section of the Combustion Institute*, Hilton Head, SC, 1996; pp 329−332.

(27) Kreith, F. *The CRC Handbook of Thermal Engineering*; CRC Press: Boca Raton, FL, 2000.

(28) CHEMKIN Collection, v.3.6: R. J. Kee, F. M. Rupley, J. A. Miller, M. E. Coltrin, J. F. Grcar, E. Meeks, H. K. Moffat, A. E. Lutz, G. Dixon-Lewis, M. D. Smooke, J. Warnatz, G. H. Evans, R. S. Larson, R. E. Mitchell, L. R. Petzold, W. C. Reynolds, M. Caracotsios, W. E. Stewart, P. Glarborg, C. Wang, and O. Adigun, Reaction Design, Inc., San Diego, CA, 2000.

(29) NIST Disclaimer: Certain commercial materials and equipment are identified in this paper to specify procedures completely. In no case does such identification imply recommendation or endorsement by the National Institute of Standards and Technology, nor does it imply that the material or equipment identified is necessarily the best available for the purpose.

(30) Glasier, G. F.; Pacey, P. D. *Nano Lett.* **2001**, *1*, 527−530.

(31) Wong, B. M.; Matheu, D. M.; Green, W. H., Jr. *J. Phys. Chem. A* **2003**, *107*, 6206−6211.

(32) Smith, J. M.; Van Ness, H. C. *Introduction to Chemical Engineering Thermodynamics*; McGraw-Hill: New York, 1987.

(33) Oberlin, A. *Carbon* **2002**, *40*, 7−24.

(34) Tatang, M. A. Direct Incorporation of Uncertainty in Chemical and Environmental Engineering Systems. Ph.D. Thesis, Department of Chemical Engineering, Massachusetts Institute of Technology, Cambridge, MA, 1995.

(35) Phenix, B. D.; Dinaro, J. L.; Tatang, M. A.; Tester, J. W.; Howard, J. B.; McRae, G. J. *Combust. Flame* **1998**, *112*, 132−146.